Migration Letters

Volume: 20, No: S6(2023), pp. 249-263

ISSN: 1741-8984 (Print) ISSN: 1741-8992 (Online)
www.migrationletters.com

Future Scenario of Spatiotemporal Changes in Land Use and Land Cover Using CA-Markov Model, GIS and Remote Sensing Applications

Ibrahim A. Farhan[1], Mohd. S. Mahafdah[2], Edlic Sathiamurthy[3], Lina A. Salameh[4], Hind Sarayreh[5]

Abstract

In Jordan's Balqa governorate, spatiotemporal changes in land cover between 1984 and 2022 were examined using satellite imagery. This study analyzed the observed and future LULC (land use and land cover) patterns, with a focusing on agricultural land areas, urban land expansion, and rapid population growth. GIS, remote sensing analysis tools, CA-Markov model were employed, and satellite images of Landsat 5 TM, 8 OLI, and 9 OLI2 for the years 1984, 1994, 2004, 2014, and 2022 were used to analyze and explore LULC characteristics. Statistical analysis were performed using the Kendall correlation matrix on observed and expected LULC. The results revealed a significant increase in the total built-up area from 16.29 km2 to 54.6 km2 during the study period with an expected sharp increase of 112.7 (106.3%) in the next four decades, i.e.2050s. The study also indicated that urban sprawl was random and accompanied by increasing demand for residential land use. In addition, there was a significant decrease in the barren land, and rangeland and arable land in favor of urban expansion with a rate of change of 40.1% (r=-0.944; p=0.001) and 38.2% (r=-0.889; p=0.001), respectively. Meanwhile, the area of mixed agricultural will continue to increase and reach 392.6 km2 (220.1%) during the period 1984-2060.This study recommends that urban management should implement a comprehensive national policy, enforcing stricter regulations for urban land use patterns, and enacting new legislation.

Keywords: *Remote sensing data, CA-Markov model, Balqa governorate, GIS application, LULC change, urban expansion.*

1. Introduction

The current world is witnessing a rapid population growth, resulting in the expansion of cities and urban areas to the detriment of lands and other spaces. This necessitated a reevaluation of land uses in many cities where planning is carried out to devise effective strategies for the future and which includes social, economic, and environmental

[1] Soil, GIS and remote sensing applications, School of Arts, Department of Geography, The University of Jordan, i.farhan@ju.edu.jo
[2] Climate Change, Sustainable Agriculture and Food Security (CCSAFS), Faculty of Agriculture, Jerash University, Jerash, Jordan.
[3] Faculty of Science and Marine Environment, University Malaysia Terengganu, Kuala Terengganu 21030, Malaysia. edlic72@gmail.com
[4] GIS and geomatics applications, School of Arts, Department of Geography, The University of Jordan, lina.slameh3@gmail.com
[5] Geography of population and services, School of Arts, Department of Geography, The University of Jordan, h.alsarayrah@ju.edu.jo

dimensions to sustain natural resources leading to the relief of pressure on the ecosystem and social services (Alqahtany, 2023).

Geographic Information Systems (GIS) and remote sensing are essential techniques for detecting and monitoring changes across different land uses. These techniques enable the creation of appropriate strategies for improved management of natural resources. Via extraction of vital important indicators that contribute towards creating a map for future prediction of land uses. This, in turn, facilitates decision-making processes that are reflected in the sustainable development of society (Rwanga, 2017).

Previous studies indicate that the main problem in urban expansion at the expense of agricultural land is due to the increase in the population at large rates, which pushes the population to expand urbanization outside the cities and the boundaries of the local administration (Said et al., 2021, Alsharif et al., 2022, Koko et al., 2022, Goshem et al., 2023). This expansion is initially unsystematic within agricultural lands, which forms a new nucleus for the process of urban expansion, and studies also indicate that villages near the main cities expand more compared to villages of size far from cities (Lambin et al., 2001).

A study in Amman, Jordan applied the Markov model to predict land cover using Landsat 5 Thematic Mapper (TM) and Landsat 8 Operational Land Imager (OLI) datasets in addition to geophysical variables. The study found that the built-up area might increase three and a half times from 1984 to 2030 (Khawaldah, 2016). In North Jordan, Irbid, remote-sensing data and field observations were used to identify and assess the contributing variables to geospatial and temporal LULC changes (Khawaldah, 2020). Classified remote sensing data also helped identify areas that could be transformed into built-up areas (Nadoushan, 2015).

Changes in LULC have been identified using different analytical models, such as statistical models, hybrid models, Markov models, hybrid models, cellular models, and evolutionary models (Mathanraj et al., 2021). Markov model is a theory, in which the projected state of a system can be modeled purely based on the immediately preceding state. Markov chain analysis describes LULC from one period to another and use this as the basis to predict future changes (Mondal et al., 2019).

This study reveals the changes in land uses, especially urban sprawl at the expense of agricultural and rangelands, and to evaluate and propose solutions to preserve and sustain agricultural land. The study area is distinguished by its geographical and climatic diversity; which plays a significant role in drawing the city's nature and the extent of its impact on surface appearances, besides other natural resources such as agricultural land, springs, and various minerals.

This study aims to identify the LULC patterns and the rate of change in agricultural land areas, population density, and distribution during the period 1984-2022. It uses the Cellular Automata (CA)-Markov model to create that assess the transformation occurs on different land use patterns, which will further benefit the land use planning of the study area.

2. Study Methodology

2.1. Study area

Balqa governorate’s located within the central region of western Jordan (Figure 1).The study area is located between 32.22º and 32.23ºN latitude and between 35.50º and 35.53ºE longitude with an altitude range from -390 meters (bsl) to 1136 meters (asl).The of Balqa governorate, cover an area of 1120 km2 (Greater Salt Municipality, 2017).

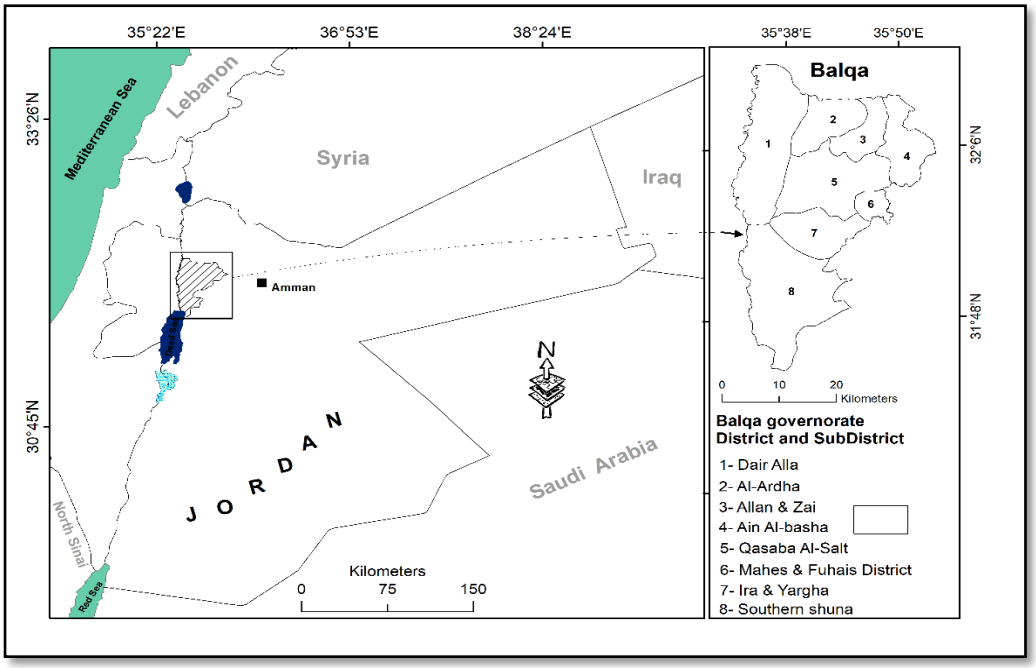

Figure 1. Map of Balqa governorate.

The study area experiences a mean annual rainfall is between 50 mm in the southwestern part and more than 500 mm in the northern part (Figure 2). It's obvious that the rainfall gradually decreases from 500 mm in the mountainous area of Balqa to less than 50 mm in the south Jordan valley. (MWI, 2010).

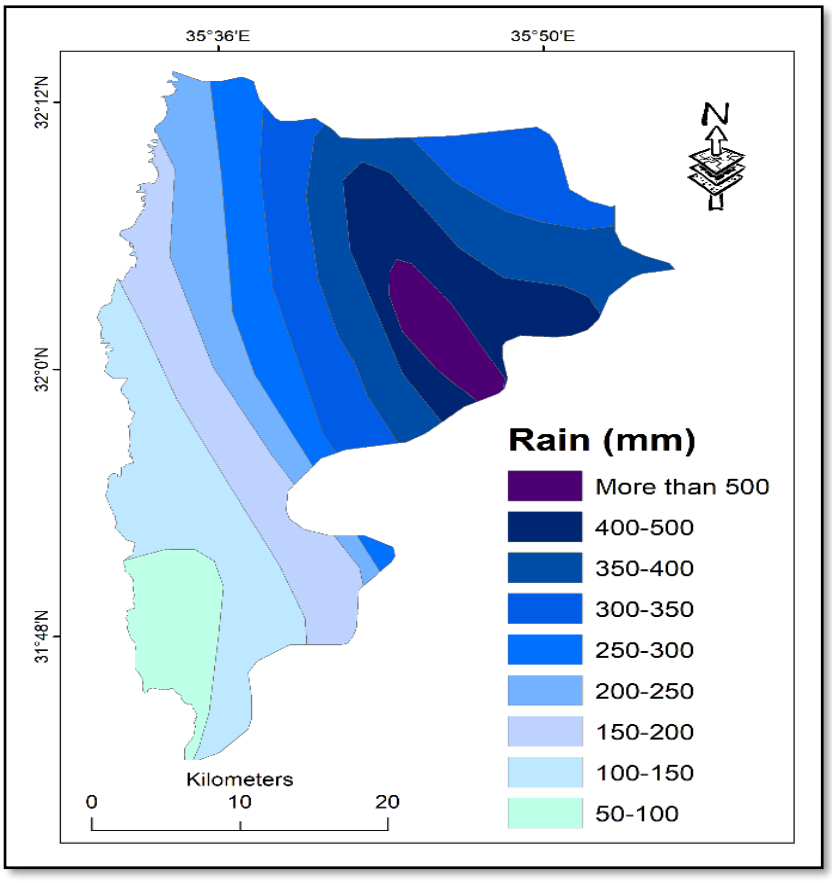

Figure 2. Map of mean annual rainfall.

According to the 2021 national population and housing census, the population of the districts was 569500, of which 305800 are males and 263700 are females Figure 3. Agriculture, including crop farming and animal husbandry, is the basis of livelihoods in the district and it is characterized by rainfed, small scale and labor-intensive activities (DOS, 2021).

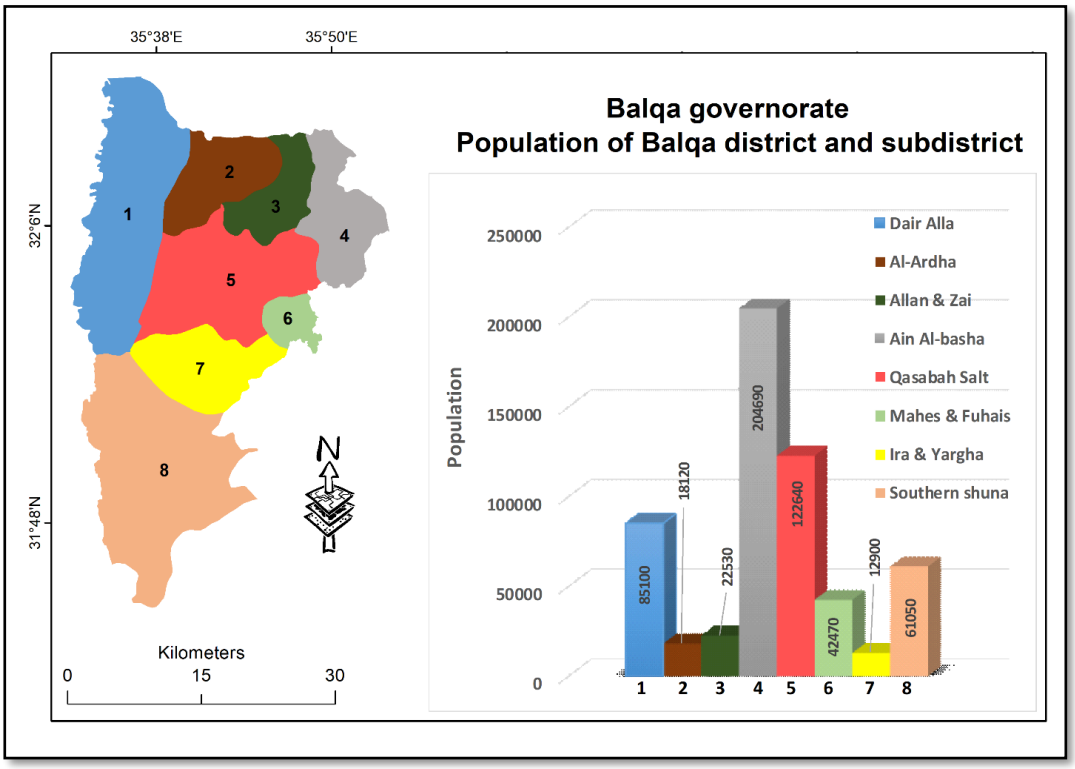

Figure 3. Estimated population of Balqa districts at the end of year 2021.

2.2. Data acquisition and image pre-processing

Landsat data were used to generate current LULC and to produce the future scenario of LULC change patterns and their future extent throughout the Balqa governorate. Satellite images for the years 1984, 1994, 2004, 2014, and 2022 were obtained from the Earth Resources Observation and Science (EROS) Center through the United State Geological Survey (USGS) Global Visualization Viewer (USGS, 2022). Cloud-free images were acquired for the spring and summer seasons (April-May and July-August) to minimize seasonal influences and also to discriminate between rangeland and irrigated crops (Table 1). Each Landsat was georeferenced to the World Geodetic System 1984 (WGS84) datum and Universal Transverse Mercator Zone 36 North (UTM-36N) coordinate system. Intensive pre-processing such as layer stacking, geo-referencing, and image enhancement was carried out to ortho-rectify the satellite images. The images were then processed in ENVI 5.3 software. Afterward, the images for the study area were extracted by clipping the study area using ArcGIS 10.8.1 software.

Table 1. Specification of Landsat 5 TM and Landsat 8/9 OLI1/2 used for classification.

Satellite type	Acquisition date	Bands/color	Spatial resolution (m)
Landsat 5 TM	15-04-1984	Visible/NIR	30x30
	05-08-1984		
	11-04-1994		
	17-08-1994		
	24-05-2004		
	11-07-2004		
Landsat 8 OLI	18-04-2014	Visible/NIR/SWIR	30x30

	08-08-2014		
Landsat 9 OLI2	16-04-2022	Visible/NIR/SWIR	30x30
	06-08-2022		

Sources: https://landsat.usgs.gov/landsat-5, 8 and 9; Where, NIR is Near Infrared and SWIR is Short Wave Infrared.

2.3. Land use/cover mapping

For producing LULC maps from Landsat satellite images, five LULC classes were identified based on fieldwork, visual interpretation using google Earth Pro, and pseudo-natural color combination for satellite images. The on-screen digitizing method was used to draw the main features from the different satellite images. The area was classified into these main classes: built-up area, barren land, rangeland and arable land, forest and mixed agriculture, and water bodies. The built-up area includes residential, commercial, industrial, educational, and recreational establishments and transportation systems (Table 2).

Table 2. Land use categories.

Code	Land use classes	Description
1	Built-up area	Continuous and discontinuous residential areas, commercial, industrial, educational, recreational establishments and transportation systems
2	Barren land	Open spaces with little or no vegetation, bare rocks and limestone.
3	Rangeland, arable lands and rainfed area	Non-irrigated arable lands, rainfed wheat in the high rainfall areas and Sparsely vegetated areas; heavily grazed open shrub and herbaceous rangeland.
4	Forest land and mixed agriculture	Permanently irrigated lands; crop irrigated permanently, areas of annual crops associated with permanent crops on the same parcel, annual crops, orchard, Pine and oak forests.
5	Water bodies	Bodies of water including agricultural ponds and dams.

2.4. CA-Markov model for LULC prediction

2.4.1 CA-Markov Model

The Markov model represents the integration of a stochastic process based on the transition probability matrices for prediction and optimal control (Agbinya, 2020). The digital map for the study area was used to illustrate the recent changes in the spatial data over time, while the Markov model was used to control spatial dynamics relying on transition probabilities, where the changes in the study area are calculated by the following equation: -

$$FX\,(X\,(tn+1) \le xn+1 \mid X\,(tn)) = xn,\ X\,(tn-1) = xn-1,..,\ X\,(t1) = FX\,(X\,(tn+1) \le xn+1 \mid X\,(tn)) = xn \ldots\ldots \text{Eq. (1)}$$

Markov chain process X (t) is the process for a particular time (t), where (tn) refers to the present time and (tn+1) defines the time for changes in the future. Similarly, the notation tn−1 is used to denote the previous changes. In mathematical terms, the definition can be expressed based on the number of stochastic processes, X (t), for any moment in time, $t1 < t2 < \cdots < tn < tn + 1$; thus, the random process will satisfy equation 1 (Memarian et al., 2012).

The equation is used to compute the probabilities of past and current states occurring by observing them as states transitioning into other states in the future, or transitioning into the same state as before. Thus, the stochastic model chain is a discrete sequence of variables, each drawn from a discrete feature space (Xianyou et al., 2020).

In other terms, the future stochastic process depends neither on its current state nor its past state. If the X[k] is the Markov chain and xn is a set of N states {x1, x2, x3, ⋯ xn}, then the transition probability matrix from state i to state j in one time instant can be expressed by equations 2 and 3 (Memarian et al., 2012).

P i, j Pr (X [k +1] = j ⎪X [k] = i)……. Eq. (2).

$$\begin{bmatrix} P_{1,1} & P_{1,2} & P_{1,3} & -- & -- & P_{1,n} \\ P_{2,1} & P_{2,2} & P_{2,3} & -- & -- & P_{2,n} \\ P_{3,1} & P_{3,2} & P_{3,3} & -- & -- & P_{3,n} \\ -- & -- & -- & -- & -- & -- \\ -- & -- & -- & -- & -- & -- \\ P_{n,1} & P_{n,2} & P_{n,3} & -- & -- & P_{n,n} \end{bmatrix} \quad \text{……. Eq. (3).}$$

2.4.2. CA-Model Validation

Model validation and assessment are necessary steps in the modeling process, especially when comparing predicting the future with the current state. Moreover, one of the most powerful models to evaluate the predicting future changes is Kappa statistics. Thus, the Markov model is used to predict future changes when the model is optimized with satisfactory performances, such as using the indices of Kappa (Kno), (Klocation), and (Kquantity). Where Kno is the overall accuracy of simulation which represents the variation of the standard Kappa index of agreement. While Klocation validates the ability of the model to predict the location, Kquantity predicts the quantity (Pontius and Schneider 2001). When the value of Indices is equal or near1 then the simulation is defined as exemplary, and if it is 0 then the simulation is considered ineffective or the consistency between the observed and simulated is imperfect. Generally, the value of Kappa is usually between 0 and 1 (Table 3). Therefore, when the value of Kappa is below 0.4 indicates less chance of a fair agreement, while the values are between 0.4 ≤ Kappa ≤ 0.6 the accuracy is moderate and when Kappa is greater than 0.6, there are small differences between observed and simulated location and almost substantial agreement indicates (Wu et al., 2008; Qiu and Lu, 2018).

Table 3: Kappa values interpretation.

Kappa value	Interpretation
< 0	Less agreement
0–0.2	Weak agreement
0.2–0.4	Fair agreement
0.4–0.6	Mild agreement
0.6–0.8	Intrinsic agreement
0.8–1.0	Almost whole agreement

The Kappa statistics method were computed as equations 4, 5 and 6(Omar et al., 2014).

K_{no} = (M(m) N(n)) / (P(p) – N(n)) ---------- Eq. (4).

$K_{location}$ = (M(m) N(m)) / (P(m) – N(m)) ---------- Eq. (5).

$K_{quantity}$ = (M(m) H(m)) / (K(m) – H(m)) ---------- Eq. (6).

Where, M(m) is the medium grid cell level information, N(n) defines no information, high consistency between grid cell-level information by (P(p), H(m) is the information of medium layer level, and the ideal grid cell-level information given heterogeneity or minimum consistency in layer-level information by K(m) means.

3. Result and Discussions

3.1. LULC classification

There are five LULC classes listed in Table (4), including Built-up (BU), Barren Area (BA), Rangeland and Arable Land (RA+AL), Forest and mixed agriculture (FL+MA),

and Water Bodies (WB). For each LULC class and year, Table (4) displays the area in km2 and the percentage of the total area covered by that class.

In 1984, RA+AL including the rainfed area covered 49.5% (537.7 km2) of the Balqa governorate area, followed by BA 37.6% (409.2 km2), FL+MA 11.3% (122.7 km2), and WB 0.1% (1 km2). In 1994, BA was the dominant LULC class which accounted for 42.6% (463 km2), followed by RA+AL at 35.2% (382.7 km2), FL+MA at 19.8% (215 km2), and WB at 0.1 (1 km2). In 2004 and 2014, more than 38% of the governorate area was occupied by RA+AL, but BA was lost. By 2022, about 38.5% (418.3 km2) of the study area was covered by FL+MA, followed by RA+AL 32.7% (355.9 km2), whereas BA and WB accounted for the lowest proportion.

Regarding the BU areas, in 1984, it covered 16.3 km2, which is 1.5% of the total area. By 2022, the area of BU had increased to 54.6 km2, which is 5.0% of the total area. Overall, the table provides information about the changes in LULC over time, which can be useful for understanding the impact of human activities on the environment.

The areal expansion of LULC changes and their distribution, for each time phase, are illustrated also in Figure 4. The study period of LULC changes is divided into five-time series as follows:(1984–1994), (1994–2004), (2004–2014), (2014–2022),and (1984–2022). The classified LULC maps of the Balqa governorate and the rate of changes are presented in Table 5.

Table 4. Area of LU/LC types in the Balqa governorate during 1984–2022.

Years (1984-2022)	**1984**		**1994**		**2004**		**2014**		**2022**	
LU/LC classes	Area (km^2)	%	Area (km^2)	%	Area (km^2)	%	Area (km^2)	%	Area (km^2)	%
BU	16.3	1.5	24.6	2.3	30.1	2.8	50.3	4.6	54.6	5.0
BA	409.2	37.6	463.5	42.6	305.8	28.1	279.8	25.7	253.7	23.3
RA+AL	537.7	49.5	382.7	35.2	521.8	48.0	417.5	38.4	355.9	32.7
FL+MA	122.7	11.3	215.0	19.8	226.8	20.9	335.7	30.9	418.3	38.5
WB	1.0	0.1	1.0	0.1	2.2	0.2	3.6	0.3	4.2	0.4
Total	1086.8	100	1086.8	100	1086.8	100	1086.8	100	1086.7	100

BU: Built-up area; BA: Barren land; RA+AL; Rangeland and arable land; FL+MA: Forest land and mixed agriculture; WB: Water bodies.

Table 5. Rate of change in LULC types in the Balqa governorate.

	Rate of change (%)				
LU/LC classes	**1984-1994**	**1994-2004**	**2004-2014**	**2014-2022**	**1984-2022**
BU	50.8	22.6	66.9	8.7	235.3
BA	13.3	-34.0	-8.5	-9.3	-38.0
RA+AL	-28.8	36.4	-20.0	-14.8	-33.8
FL+MA	75.2	5.5	48.0	24.6	241.0
WB	5.6	113.9	62.2	17.6	330.9

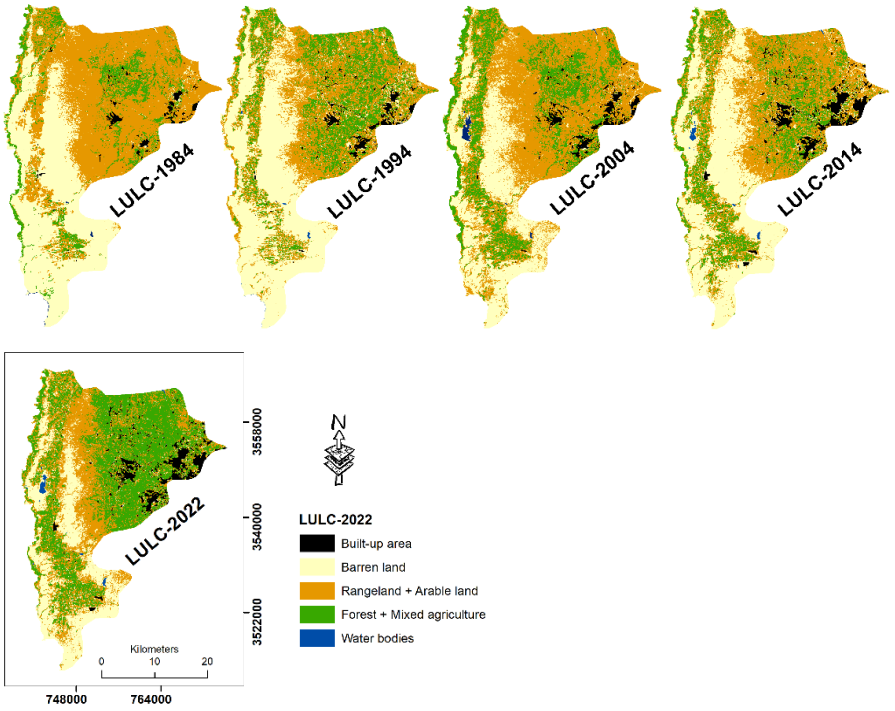

Figure 4. LULC of Balqa districts.

3.2. LULC changes between 1984 and 2022

The majority of the rural inhabitants rely on agriculture, especially crop cultivation. The percentage of land that has been gradually raised from1984 to 2022, and used for crop production (mixed agriculture). On the other hand, the entire area of BA decreased at an average rate of 4.1 km2/year with a rate of change of -38% (Tables4 and 5).

Mixed agriculture and rangeland areas have transformed into built-up areas, including rainfed agriculture areas in the surrounding Salt city. Mixed agriculture has transformed into other land use types. The built-up areas percentage has risen successively over the study time. It grew from 1.5% in 1984 to 5% in 2022 with a progressive rise. Nonetheless, the percentage of mixed agriculture share was 122.7 km2 (11.3%), and 418.3 km2 (38.5%) in 1984, and 2022, respectively (Table 4). The rangeland and arable lands of the governorate have been gradually declining at an annual rate of 4.8 km2/year with a rate of change equal to -33.8 between 1984 and 2022 (Table 5). Based on the current LULC change study, a slight rise happened in the water bodies from 1 km2 (0.1%) in 1984 to 4.2 km2 (0.4%) in 2022, respectively (Table 4).

Image divergence is among the different strategies that have been used to detect LULC change. The detection of isotropy changes between 1984 and 2022 describes the magnitude of land cover change over the past four decades (Table 7). A positive estimate of image discrimination shows an increase in the spatial neighborhood for the areas of forest, mixed agriculture land, built-up and water bodies. Whereas the remaining land units, named ranges, arable and barren lands, have depicted a declining trend while there is an increase in urban built-up areas and mixed agriculture (Table 6). The present study confirmed the highest percentage change in the RA+AL (Table 7), and the extent of these changes was 63.11%, followed by WB (47.57%), BA (44.09%), FL+MA (30.76%), and BU area (7.03%) over the whole study periods. The LULC transformation matrix analysis of 38 years from 1984 to 2022 of the study landscapes is shown in Table 6.

Table 6. Change detection matrix for LULC types during the period 1984–2022.

	LULC in 1984 (area in km^2)					
LULC Class	BA	BU	FL+MA	RA+AL	WB	Row Total

LULC in 2022 (area in km^2)	BA	**228.74**	0.18	4.94	19.44	0.41	253.72
	BU	3.15	**15.17**	3.58	32.74	0.00	54.64
	FL+MA	45.96	0.48	**84.94**	286.89	0.01	418.27
	RA+AL	127.92	0.46	29.10	**198.38**	0.04	355.90
	WB	3.39	0.02	0.10	0.26	**0.51**	4.29
	Column Total	409.16	16.32	122.67	537.71	0.97	1086.83
	Class changes	180.42	1.15	37.73	339.33	0.46	
	Image difference	-155.44	38.32	295.61	-181.81	3.32	

Table 7. Transformation matrix for LULC 1984–2022.

		LULC in 1984 (area %)					
	LULC Class	BA	BU	FL+MA	RA+AL	WB	Row Total
LULC in 2022 (area in km^2)	BA	**55.91**	1.13	4.03	3.62	42.39	100
	BU	0.77	**92.97**	2.92	6.09	0.01	100
	FL+MA	11.23	2.96	**69.24**	53.35	0.57	100
	RA+AL	31.26	2.79	23.73	**36.89**	4.60	100
	WB	0.83	0.15	0.09	0.05	**52.43**	100
	Column Total	100	100	100	100	100	
	Class changes	44.09	7.03	30.76	63.11	47.57	
	Image difference	-38.0	234.8	241.0	-33.8	341.1	

3.3. The major drivers of LULC change

The agricultural sector in the Balqa governorate shows promising signs of development based on the available data and indicators. Specifically, the percentage of cultivated areas in Balqa governorate represents approximately 25% of the total cultivated areas across the Kingdom. The Kingdom's total cultivated area is estimated to be 241,223.4 hectares, which is about 2.7% of the total area of the Kingdom (89,342 km2). In terms of cultivated areas in the Kingdom, the area planted with fruit trees in the Balqa governorate constitutes 20% of the total area devoted to fruit cultivation. Similarly, the area planted with vegetables in Balqa governorate accounts for 25% of the total area devoted to vegetable cultivation across the Kingdom. Whereas, the results of the analysis revealed the rates of change were significantly decrease ($r=-0.37$; $p=0.006$) in cultivation areas which include; cereal, vegetable, and fruit trees crops, such as wheat, barley, tomato, potato olives, grapes, pomegranates, etc. This is the case in Ira, Yargha, Southern Shuna, Deir Alla,Ain Albasha, and Alfuheis, respectively(MOA, 2022).

The primary field crop in the Balqa governorate is barley, with particular emphasis on its cultivation in low to medium-slope areas such as Ira and Yargha. The protected and exposed vegetables in Shuna and Ain Albasha constituted about 8% of the area of the governorate in 1997, and decline to reach 4.8% of the area in 2021(Figure 5). The rate of change in the area of agricultural lands is -40.35 during the period (1997-2021)as shown in Figure 5. The reasons behind the prominence of barley cultivation in the Balqa governorate are multifaceted. These include fluctuations in rainfall patterns, small agricultural holdings resulting from property fragmentation due to the presence of multiple partners on registration deeds, and the high cost of agricultural production requirements. Additionally, the high cost of land reclamation in the governorate can be attributed to the steep and rocky nature of the geographical land, as well as the challenges associated with marketing agricultural products.

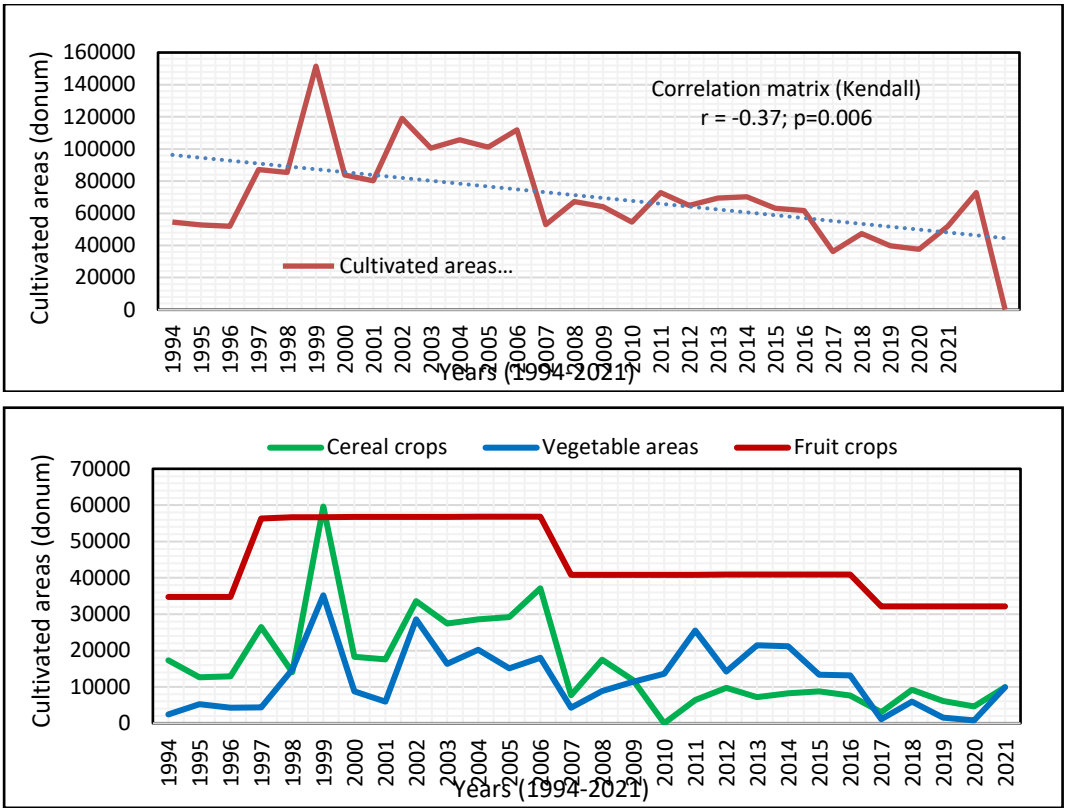

Figure 5. a; Total cultivated areas and b; Crop types patterns from 1994 to 2021 in Balqa governorate (Note: 1donum equal to 10 hectares).

3.4. Validation of CA- Markov for LULC modeling and prediction

Table 8 displays the Kappa statistics, indicating a high level of agreement and consistency between the simulated and observed values of LULC classes with minor differences. Kno, Klocation, and Kstandardare above 0.73, 0.78, and 0.67 respectively. On the other hand, Kappa indices of the agreement were used to confirm different changes that could happen in the LULC maps of years 2030, 2040, 2050, and 2060. The outcomes suggest that the CA-Markov model is an effective tool for simulating and analyzing different LULC changes in the aforementioned years. Thus, the model is considered reliable and trustworthy in predicting future LULC change.

Table 8. Summary of model validation.

Maps used for validation	Observed LULC	Predicted LULC	Compatibility degrees (%)	Kappa indices (0-1)		
				K_{no}	$K_{location}$	$K_{standard}$
1984 - 1994	2004	2004	79.5	0.76	0.78	0.70
1994 - 2004	2014	2014	81.8	0.80	0.82	0.74
2004 -2014	2022	2022	78.5	0.73	0.78	0.67

3.5. Predictable LULC changes for next four decades

The LULC patterns for the years 2030, 2040, 2050, and 2060 have been projected based on the CA-Markov chain mode. According to Tables9a, 9b, 9c, and 9d, the transitional matrices for LULC probability between 2014-2022, 2004-2022, 1994-2022, and 1984-2022were analyzed using the Markovian transition estimator. Columns and rows categories of the tables entered LULC classes for each time period. According to the data presented in Table 9a, there is a matrix indicating the probability of changes in the LULC class by the year 2030, as well as the corresponding gains and losses of each category. The forest and mixed agriculture areas are expected to experience the most significant increase, with a gain of 64.01%. On the other hand, rangeland will suffer the most significant loss, with a decrease of 61.16%. It is projected that the forest and mixed

agricultural land will cover 76.31% of the total area, while rangeland will transform into mixed agricultural and barren land, covering 57.33% and 3.18%, respectively. Future changes in rangeland to mixed agricultural and barren land are 57.33% and 3.18% respectively. The barren land will lose44.48% of its land use.

Table 9a: Probability of transition class for LULC 2014-2022 to simulate 2030.

LULC Classes	BU	BA	RA+AL	FL+MA	WB	Probability of Changing by 2030	
						Total	Loss
BU	**0.9994**	0	0	0	0.0006	1	0.0006
BA	0.0035	**0.5552**	0.3789	0.0599	0.0025	1	0.4448
RA+AL	0.0062	0.0318	**0.3885**	0.5733	0.0003	1	0.6116
FL+MA	0.0018	0.0373	0.1976	**0.7631**	0.0002	1	0.2369
WB	0.0402	0.075	0.0146	0.0069	**0.8633**	1	0.1367
Total	1.0511	0.6993	0.9796	1.4032	0.8669	**5**	
Gain	0.0517	0.1441	0.5911	0.6401	0.0036		

Table 9b: Probability of transition class for LULC 2004-2022 to simulate 2040.

LULC Classes	BU	BA	RA+AL	FL+MA	WB	Probability of Changing by 2040	
						Total	Loss
BU	**0.998**	0	0.0005	0.0002	0.0013	1	0.002
BA	0.0092	**0.6668**	0.259	0.0638	0.0011	1	0.3331
RA+AL	0.0356	0.0752	**0.4204**	0.468	0.0007	1	0.5795
FL+MA	0.0139	0.0418	0.2672	**0.6765**	0.0006	1	0.3235
WB	0	0.2356	0.0604	0.0047	**0.6993**	1	0.3007
Total	1.0567	1.0194	1.0075	1.2132	0.703	**5**	
Gain	0.0587	0.3526	0.5871	0.5367	0.0037		

Table 9c: Probability of transition class for LULC 1994-2022 to simulate 2050.

LULC Classes	BU	BA	RA+AL	FL+MA	WB	Probability of Changing by 2050	
						Total	Loss
BU	**0.977**	0.0022	0.0103	0.0091	0.0015	1	0.0231
BA	0.0139	**0.5013**	0.3624	0.1153	0.0071	1	0.4987
RA+AL	0.0456	0.0348	**0.3909**	0.5283	0.0004	1	0.6091
FL+MA	0.0309	0.0309	0.1927	**0.7451**	0.0004	1	0.2549
WB	0.0018	0.1691	0.0216	0.0045	**0.8031**	1	0.197
Total	1.0692	0.7383	0.9779	1.4023	0.8125	**5**	
Gain	0.0922	0.237	0.587	0.6572	0.0094		

Table 9d: Probability of transition class for LULC 1984-2022 to simulate 2060.

LULC Classes	BU	BA	RA+AL	FL+MA	WB	Probability of Changing by 2060	
						Total	Loss
BU	**0.9291**	0.0117	0.028	0.0292	0.002	1	0.0709
BA	0.0077	**0.5567**	0.3139	0.1133	0.0084	1	0.4433
RA+AL	0.0606	0.0348	**0.3726**	0.5315	0.0005	1	0.6274
FL+MA	0.0301	0.0378	0.2416	**0.6896**	0.0009	1	0.3104
WB	0	0.4179	0.052	0.0064	**0.5237**	1	0.4763
Total	1.0275	1.0589	1.0081	1.37	0.5355	**5**	
Gain	0.0984	0.5022	0.6355	0.6804	0.0118		

According to Table 9d, there is a 92.91% chance of built-up land changing to other built-up land by 2060. In contrast, the probability of built-up land changing to barren land,

rangeland, and mixed agriculture land is only 1.17%, 2.8%, and 2.9%, respectively. This means that a significant amount of rangeland, barren land, and mixed agriculture land is at risk of being lost, with percentages of 62.74%, 44.33%, and 31.04%, respectively. Furthermore, the analysis predicts that about 6% of rangeland will convert to built-up land based on the predicted map.

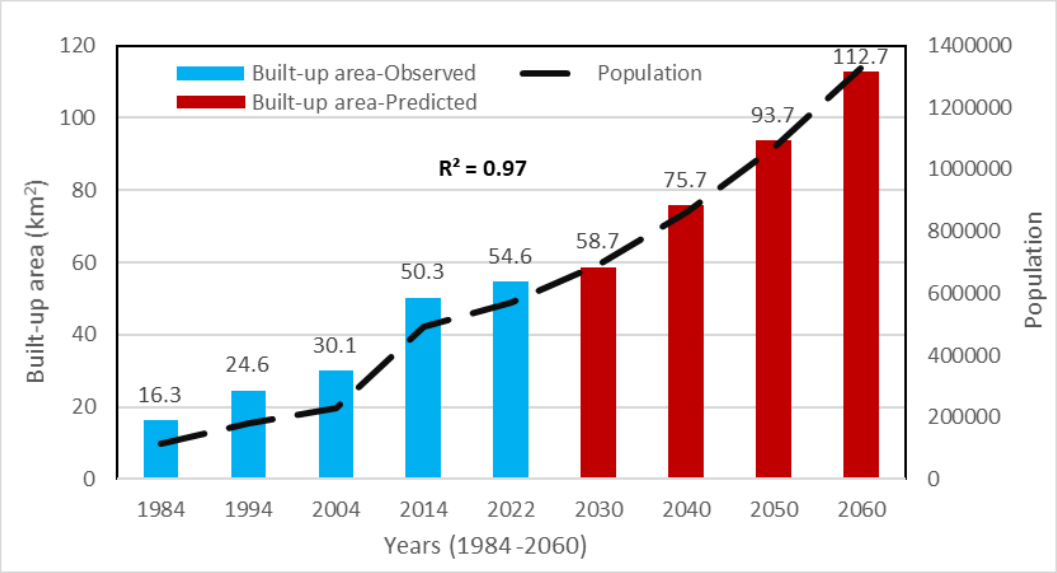

Figure 6. Trend analysis for increases in the built-up area and population.

Figure 6 illustrates a general trend of the built-up area changes in the Balqa governorate, which is expected to continue from 2030 to 2060.The population growth rate of the Balqa governorate was calculated using the exponential equation (Agung, 1993). At the end of 2021, the population of Balqa was 569.5thousand and is anticipated to rise to 1.33 million by 2060, indicating an annual growth rate of 2.2%. This represents a 133.6% increase in population over the next four decades. The projected increase in the built-up area is 106.3%, which aligns well with the anticipated population growth. Furthermore, there has been a substantial increase in built-up area over the years, while the population trend line displays a consistent upward pattern with a coefficient of determination (R2) value of 0.97. As a result, the predicted value is highly reliable and closely aligned with actual data. According to Figure 7, it can be seen that the built-up area has significantly increased over the years. The area occupied by built-up area was 16.3 km2 in 1984, which increased by 235.3% to 54.6 km2in 2022, and then increased by 106.3% to 112.7km2 in 2060 (Table 10).

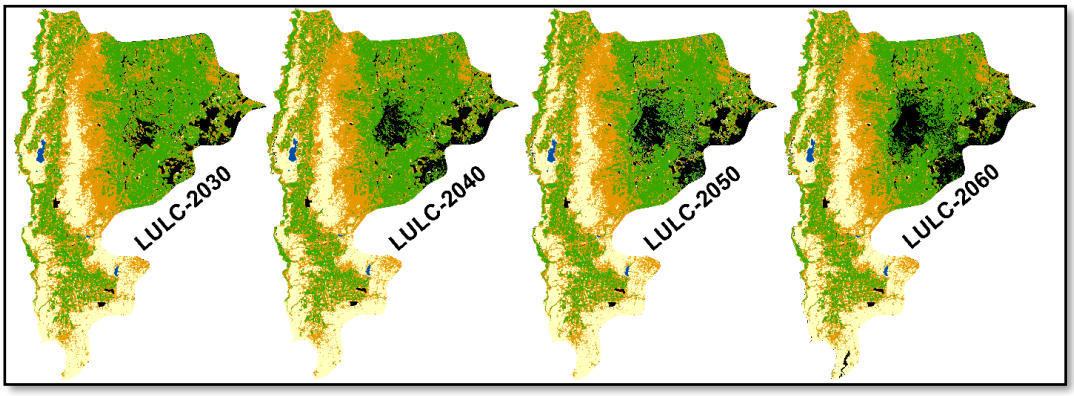

Figure 7. Predicted LULC changes in Balqa governorate for the period from 2030 to 2060.

The correlation matrix of LULC in Table 10 shows that the built-up area is significantly correlated positively with water bodies and negatively with barren and rangeland areas. The water bodies are negatively correlated with barren land and rangeland areas.

Table 10. Correlation matrix (Kendall) (r) and (p-values) of LULC during the period of 1984 to 2060.

Variables	BU		BA		RA+AL		FL+MA		WB	
	r	p-value	r	p-value	RA+AL	p-value	r	p-value	r	p-value
BU	**1**	**0**	**-0.944**	**0.001**	**-0.889**	**0.001**	0.500	0.076	**0.833**	**0.002**
BA	**-0.944**	**0.001**	**1**	**0**	**0.833**	**0.002**	-0.444	0.118	**-0.778**	**0.005**
RA+AL	**-0.889**	**0.001**	**0.833**	**0.002**	**1**	**0**	-0.389	0.175	**-0.722**	**0.009**
FL+MA	0.500	0.076	-0.444	0.118	-0.389	0.175	**1**	**0**	**0.556**	**0.048**
WB	**0.833**	**0.002**	**-0.778**	**0.005**	**-0.722**	**0.009**	**0.556**	**0.048**	**1**	**0**

***Values in bold are different from 0 with a significance level alpha=0.05**

Rangelands in the western part of the governorate constitute 32.7% of the total area while most of it is used as rainfed that is planted with barley and wheat for flour. Where the cultivated area of wheat and barley constitutes 93.6% of the total cultivated areas of cereal crops in this zone (MOA, 2022). Barley is cultivated for a straw to support grazing herds of sheep. The non-cultivated areas are also heavily grazed and susceptible to soil erosion (Farhan and Al-Bakri, 2019).The eastern areas of the governorate, which receive a higher amount of rainfall as shown in Figure 2, are mainly used for cultivating olives, and fruit and vegetable crops. The areas under forest and trees have increased slightly as many are now protected under national conservation programs. Other areas are owned by residents and presented as agricultural tenure. The irrigated areas constitute 5.4% of the total area of Balqa governorate especially in the eastern part (Al-Baqa'a area) and western part (southern Shuna) because these regions are characterized by moderate temperatures in the winter and hot in the summer. Also, the water resource in the southern Shuna area is available through the King Abdullah Canal (KAC). However, it was noticed in the last decade that the agricultural pattern in the southern Shuna region has gradually shifted to palm cultivation due to the economic value of this crop besides its ability to withstand drought and salinity that is concentrated in the soil.

According to the results of the probability of transition classes for the years 2030, 2040, 2050, and 2060, it was found that the land cover of rangeland and barren areas might decline at a rate of 60.7 and 42.9, respectively. Meaning that urbanization will devour the largest quantities of arable and rangeland in the future (Tables 9 and 10). Additionally, with the expansion in the built-up area, there was a conversion of rainfed areas to irrigated areas because of profit-oriented farming practices during the period from 1984 to 2022.Moreover, due to climatic changes, it is probable that there will be a slight decrease of 28.1% in the areas of forests and irrigated crops. The previous studies indicated that the annual rainfall rate has decreased by 10% from the long-term rate of the Balqa Governorate. According to the predicted results, the irrigated area will continue to increase due to high economic returns for this LULC type. Finally, the governorate as an arid and semi-arid area is highly sensitive to adverse effects on environmental sustainability (Farhan et al., 2012). Therefore, appropriate management for land use plans and utilization is needed, with emphasis on controlling the encroachment of built-up areas (residential, commercial, and industrial) on rangeland, forest, and mixed agriculture. Figures 4 and 8 showed the development of the built-up area in the governorate from 1984 to 2060.

4. Conclusion

Multi-temporal Landsat imagery in 1984, 1994, 2004, 2014, and 2022 were used to produce LULC maps which were further used in the CA-Markov process to simulate the future spatial and temporal changes of LULC. GIS analysis and CA- Markov model

indicated a notable decline in barren, rangeland and arable land and a considerable increase of built-up area in Balqa governorate during the period (1984-2060).However, results revealed that the built-up area expanded from only 16.29 km² in 1984 to 54.6 km² in 2022, with a rate of change of 235.3%. Also, the simulation indicated that the built-up area will continuously increase and reach 112.7 km² in 2060, where this expansion will be at the expense of rangeland and arable land. This change in the built-up area is caused by the rapid population increase, with a population growth rate of2.2, resulting from immigration and internal migration. Therefore, the study of rapid urbanization especially spatiotemporal changes in land use has become increasingly critical for understanding urban dynamics and environmental impacts, as well as guiding sustainable urban development. In the end, The CA-Markov model and GIS application proved to be powerful tools for analyzing LULC dynamic change and predicting future scenarios.

References

1. Agbinya, J. I. (2020). Markov Chain and its Applications an Introduction.
2. Agung, I. N. (1993). Identical population estimates using the exponential and geometric growth functions, Majalah Demografi Indones, 20(40), 69-74.
3. Alqahtany, A. (2023). GIS-based assessment of land use for predicting increase in settlements in Al Ahsa Metropolitan Area, Saudi Arabia for the year 2032. Alexandria Engineering Journal, 62, 269–277.
4. Alsharif, M., Alzandi, A. A., Shrahily, R., & Mobarak, B. (2022). Land Use Land Cover Change Analysis for Urban Growth Prediction Using Landsat Satellite Data and Markov Chain Model for Al Baha Region Saudi Arabia. Forests, 13(10).
5. DOS (Department of Statistics), (2021). Amman, Jordan.
6. Farhan, I. A., & Al-Bakri, J. T. (2012). Use of GIS and Remote Sensing to Assess Soil Erosion in an Arid to Semiarid Basin in Jordan. Proceedings of the International Con-Ference on Sediment Transport: Modeling in Hydrologi.
7. Farhan, I. A., & Al-Bakri, J. T. (2019). Detection of a Real Time Remote Sensing Indices and Soil Moisture for Drought Monitoring and Assessment in Jordan. Open Journal of Geology, 09(13), 1048–1068.
8. Goshem, G. K., Sahile, W. T., Shifaw, S. A., & Abidin, M. R. Analyzing and Predicting Land Use and Land Cover Changes with an Integrated CA-Markov Model: A Spatiotemporal Perspective in Case of Chuko Town and Surroundings, Sidama Region, Ethiopia.
9. Greater Salt Municipality, 2017, Records and reports in the GIS department. Balqa, Jordan.
10. Hassan, M. M., & Nazem, M. N. I. (2016). Examination of land use/land cover changes, urban growth dynamics, and environmental sustainability in Chittagong city, Bangladesh. Environment, Development and Sustainability, 18(3), 697–716.
11. Khawaldah, H. A. (2016). A Prediction of Future Land Use/Land Cover in Amman Area Using GIS-Based Markov Model and Remote Sensing. Journal of Geographic Information System, 08(03), 412–427.
12. Khawaldah, H. A., Farhan, I., & Alzboun, N. M. (2020). Simulation and prediction of land use and land cover change using GIS, remote sensing and CA-Markov model. Global Journal of Environmental Science and Management, 6(2), 215–232.
13. Koko, A. F., Han, Z., Wu, Y., Abubakar, G. A., & Bello, M. (2022). Spatiotemporal Land Use/Land Cover Mapping and Prediction Based on Hybrid Modeling Approach: A Case Study of Kano Metropolis, Nigeria (2020–2050). Remote Sensing, 14(23), 6083.
14. Lambin, E. F., Fischer, G., Turner, B. L., Geist, H. J., Agbola, S. B., Angelsen, A., Bruce, J. W., Coomes, O. T., Dirzo, R., Unther Fischer, G. U., Folke, C., George, P. S., Homewood, K., Imbernon, J., Leemans, R., Li, X., Moran, E. F., Mortimore, M., … Xu, J. (2001). The causes

of land-use and land-cover change: Moving beyond the myths. In Global Environmental Change (Vol. 11).

15. Mariye, M., Jianhua, L., & Maryo, M. (2022). Land use and land cover change, and analysis of its drivers in Ojoje watershed, Southern Ethiopia. Heliyon, 8(4).
16. Mathanraj, S., Rusli, N., & Ling, G. H. T. (2021). Applicability of the ca-markov model in land-use/ land cover change prediction for urban sprawling in batticaloa municipal council, Sri Lanka. IOP Conference Series: Earth and Environmental Science, 620(1).
17. Memarian, H., Kumar Balasundram, S., bin Talib, J., Teh Boon Sung, C., Mohd Sood, A., & Abbaspour, K. (2012). Validation of CA-Markov for Simulation of Land Use and Cover Change in the Langat Basin, Malaysia. Journal of Geographic Information System, 04(06), 542–554.
18. MOA (Ministry of Agriculture), (2022). Amman, Jordan.
19. Mondal, S., Sharma, M., Kappas, N. M., & Garg, P. K. (2019). Ca markov modeling of land use land cover dynamics and sensitivity analysis to identify sensitive parameter(s). International Archives of the Photogrammetry, Remote Sensing and Spatial Information Sciences - ISPRS Archives, 42(2/W13), 723–729.
20. MWI (Ministry of Water and Irrigation, Jordan), (2010). National Water Master Plan of Jordan, GTZ, Framework of cooperation between the Ministry of Water and Irrigation and GTZ,1-97, Amman, Jordan.
21. Nadoushan, M., Soffianian, A., & Alebrahim, A. (2015). Modeling Land Use/Cover Changes by the Combination of Markov Chain and Cellular Automata Markov (CA-Markov) Models. Journal of Earth, Environment and Health Sciences, 1(1), 16.
22. Omar, N. Q., Ahamad, M. S. S., Wan Hussin, W. M. A., Samat, N., & Binti Ahmad, S. Z. (2014). Markov CA, Multi Regression, and Multiple Decision Making for Modeling Historical Changes in Kirkuk City, Iraq. Journal of the Indian Society of Remote Sensing, 42(1), 165–178.
23. Pontius, R. G., & Schneider L. C. (2001). Modeling land-use change in the Ipswich watershed, Massachusetts, USA, Agriculture, Ecosystems & Environment, Volume 85, Issues 1–3, 83-94.
24. Said, M., Hyandye, C., Komakech, H. C., Mjemah, I. C., & Munishi, L. K. (2021). Predicting land use/cover changes and its association to agricultural production on the slopes of Mount Kilimanjaro, Tanzania. Annals of GIS, 27(2), 189-209.
25. Qiu, Y., & Lu, J. (2018). Dynamic simulation of Spartina alterniflora based on CA-markov model-a case study of Xiangshan bay of Ningbo city, China. Aquatic Invasions, 13(2), 299–309.
26. Rwanga, S. S., & Ndambuki, J. M. (2017). Accuracy Assessment of Land Use/Land Cover Classification Using Remote Sensing and GIS. International Journal of Geosciences, 08(04), 611–622.
27. USGS (United States Geological Survey), (2022). United State.
28. Wu, X.Q., Hu, Y.M., He, H.S. & Bu, R.C., (2008). Accuracy evaluation and its application of SLEUTH urban growth model. Geomatics.
29. Xianyou, P., Malin S., & Xiongfeng P. (2020). in Sustainable Marine Resource Utilization in China.